lnc-MICAL2-1 sponges miR-25 to regulate DKK3 expression and inhibits activation of the Wnt/β-catenin signaling pathway in breast cancer

JIA YAO[1*], GUANQIAO LI[1*], MINFENG LIU[2*], SHIPING YANG[3], HUILUAN SU[3] and CHANGSHENG YE[1]

[1]The First School of Clinical Medicine, Southern Medical University; [2]Department of General Surgery-Breast Center, Nanfang Hospital of Southern Medical University, Guangzhou, Guangdong 510650; [3]Department of Radiotherapy, Hainan General Hospital, Haikou, Hainan 570311, P.R. China

Received May 17, 2021; Accepted October 19, 2021

DOI: 10.3892/ijmm.2021.5078

Abstract. The Dickkopf 3 (DKK3) protein antagonizes the Wnt receptor complex in the Wnt signaling pathway; however, to date, there have been no relevant studies investigating its upstream regulatory mechanism in breast cancer (BC), to the best of our knowledge. The present study aimed to explore whether long non-coding RNA MICAL2-1 (lnc-MICAL2-1) sponged microRNA (miR)-25 to regulate DKK3 and inhibit activation of the Wnt/β-catenin signaling pathway. The Atlas of non-coding RNA in Cancer database was used to measure the expression levels of lnc-MICAL2-1 and their correlation with DKK3 expression levels. In addition, cell proliferation, invasion and migration were determined following the silencing or overexpression of lnc-MICAL2-1. The binding between lnc-MICAL2-1 and miR-25, or miR-25 and DKK3 was verified using RNA pull-down and dual-luciferase reporter assays. The effects of overexpression or knockdown of lnc-MICAL2-1 on DKK3 expression and the Wnt signaling pathway were further evaluated in a nude mouse xenograft model. The results revealed that, compared with in adjacent normal tissue, the expression levels of lnc-MICAL2-1 were downregulated in BC tissues, and the expression levels of lnc-MICAL2-1 were found to be positively correlated with DKK3 expression. The overexpression of lnc-MICAL2-1 in BC cells upregulated the mRNA expression levels of DKK3 and inhibited their proliferation. Results from the RNA pull-down and dual luciferase reporter assays validated that lnc-MICAL2-1 could bind to miR-25, which targets DKK3. The *in vivo* experimental data demonstrated that lnc-MICAL2-1 inhibited tumor growth via regulating the Wnt signaling pathway. In conclusion, the findings of the present study highlighted a novel molecular mechanism through which lnc-MICAL2-1 may regulate the DKK3-mediated Wnt signaling pathway in BC, highlighting potential targets for the treatment of the disease.

Correspondence to: Professor Changsheng Ye, The First School of Clinical Medicine, Southern Medical University, 1023-1063 Shatai South Road, Baiyun, Guangzhou, Guangdong 510650, P.R. China
E-mail: yechsh2006@126.com

*Contributed equally

Key words: long non-coding RNA-MICAL2-1, breast cancer, microRNA-25, Dickkopf 3, Wnt signaling pathway

Introduction

Breast cancer (BC) is the most common type of cancer among women worldwide, and the leading cause of cancer-associated mortality. According to the global cancer burden data released by the International Agency for Cancer Research of the World Health Organization, the number of new BC cases worldwide reached 2.26 million in 2020; this was the first time that BC cases surpassed the number of lung cancer cases (2.21 million) to become the most common type of cancer in the world (1). Therefore, it is necessary to determine the underlying molecular mechanisms of the occurrence and development of BC to develop effective methods for early diagnosis and treatment.

Dickkopf (DKK) protein family members, which consist of DKK1-4, as well as DKK3-related proteins, are secretory proteins (2). The DKK proteins are glycoproteins composed of 255-355 amino acids, which contain a signal sequence and two conserved cysteine-rich domains (3). DKK3 has been discovered to act as a tumor suppressor gene (4), and physiologically functions as an antagonist of the Wnt receptor complex in the Wnt signaling pathway; therefore, it can inhibit the Wnt signaling pathway (5). When DKK3 is inactivated, the Wnt protein binds to its receptor and excessive activation of this signaling pathway can lead to tumorigenesis (5,6). The expression levels of DKK3 have been found to be downregulated in numerous types of cancer cells, including melanoma, gallbladder cancer and BC (7,8), and its overexpression was discovered to inhibit the proliferation of cancer cells. However, the upstream regulatory mechanism of DKK3 in BC remains to be clarified, to the best of our knowledge.

MicroRNAs (miRNAs/miRs) are a type of non-protein coding RNA, 19-25 nucleotides in length, which play a variety of regulatory roles in the processes of cell proliferation and

development (9). miRNAs bind with the 3'-untranslated regions of their target mRNA in a complete or incomplete complementary manner, resulting in a reduction in translation or cleavage of the target mRNA (10). Multiple studies have shown that the expression levels of miR-25 were significantly upregulated in a variety of tumor tissues and cells, which could promote cell invasion and proliferation by targeting DKK3 (11,12). However, whether miR-25 can target DKK3 in BC has not been reported, to the best of our knowledge.

Long non-coding RNAs (lncRNAs) are another type of non-coding RNA that are >200 nucleotides in length and lack protein-coding ability. Previous studies have shown that lncRNAs are associated with the occurrence and development of numerous types of human disease, including cancer and Alzheimer's disease (13,14). In addition, studies have demonstrated that lncRNA acts as a competitive endogenous RNA (ceRNA) (15-17). For example, hepatocellular carcinoma upregulated lncRNA HULC was found to act as an endogenous sponge of miR-372, downregulating its expression, thereby reducing the inhibitory effect on the translation of its target genes (18).

The present study aimed to investigate the role of the lnc-MICAL2-1/miR-25/DKK3 signaling axis in BC. First, the expression levels of lnc-MICAL2-1 and DKK3 in BC tissues were analyzed using data obtained from The Cancer Genome Atlas (TCGA). Cell proliferation, invasion and migration were determined following the knockdown or overexpression of lnc-MICAL2-1. RNA pull-down and dual-luciferase reporter assays verified the targeting relationship between lnc-MICAL2-1 and miR-25, and between miR-25 and DKK3. In addition, the effects of the overexpression or knockdown of lnc-MICAL2-1 on DKK3 expression and the Wnt signaling pathway were further evaluated in a nude mouse xenograft model. Taken together, the results of the present study indicated that the lnc-MICAL2-1/miR-25/DKK3 signaling axis may play an important role in BC, suggesting that the activation of lnc-MICAL2-1/DKK3 or inhibition of miR-25 may be beneficial to the treatment of BC.

Materials and methods

Bioinformatics analysis. GeneCards (genecards.org/) database was used to explore the upstream regulatory mechanism of DKK3 in tumor cells. Prediction of lncRNA and miRNA, and miRNA and target gene binding sites was performed using TargetScan (targetscan.org/vert_72/) and miRanda (microrna.org/microrna/home.do) databases. The Atlas of non-coding RNAs in Cancer (TANRIC) database (ibl.mdanderson.org/tanric/design/basic/download.html), which is an interactive data analysis and visualization platform (19), was used to analyze the expression of lnc-MICAL2-1 in BC tissues and calculate the correlation coefficient between lnc-MICAL2-1 and DKK3 expression, which was subsequently displayed as a scatter diagram. In addition, TANRIC was used to study the relationship between lnc-MICAL2-1 expression, clinical characteristics and overall survival in BC. The corresponding clinical data of the patients in TANRIC were obtained from The Cancer Genome Atlas (TCGA) data portal (portal.gdc.cancer.gov/; normal, n=105; tumor, n=837).

Cell lines and culture. MDA-MB-231, MCF-7 and 293T cells cell lines were purchased from the American Type Culture Collection and cultured as described previously (20). MDA-MB-231 and MCF-7 cells were cultured in DMEM (Invitrogen; Thermo Fisher Scientific, Inc.) supplemented with 10% FBS (Gibco; Thermo Fisher Scientific, Inc.). 293T cells were cultured in DMEM containing 10% FBS, 2 mM L-glutamine and 50 μg/ml gentamicin. All cells were cultured at 37˚C in a humidified incubator with 5% CO_2.

Cell transfection. miR-25 mimics (5'-AGGCGGAGACUU GGGCAAUUG-3'), miR-25 inhibitor (5'-CAAUUGCCCAAG UCUCCGCCU-3'), miR-25 mimics control (5'-UUGUACUAC ACAAAAGUACUG-3') and miR-25 inhibitor control (5'-CAG UACU-UUUGUGUAGUACAA-3') were purchased from Sangon Biotech Co., Ltd. Cells were seeded ($4x10^5$ cells/well) into 6-well cell culture plates containing 2 ml complete medium. Ay 50-80% confluence, MCF-7 cells were transfected with miR-25 mimics (50 nM), miR-25 mimics control (50 nM), miR-25 inhibitor (100 nM) or miR-25 inhibitor control (100 nM) using riboFECT CP Transfection kit (Guangzhou RiboBio Co., Ltd.) at 37˚C for 48 h. pcDNA3.1/V5-His-TOPO vector (Invitrogen; Thermo Fisher Scientific, Inc.) was used to construct the lnc-MICAL2-1 overexpression and knockdown vectors. pcDNA3.1/V5-His-TOPO empty vector was used as the overexpression negative control. The sequences of the shRNAs were as follows: sh-lnc-MICAL2-1 (2 μg; 5'-AATGGCAAA CACTGAGCTGCT-3'), sh-NC (2 μg; 5'-TTCTCCGAACGT GTCACGT-3'). Vectors (2 μg) were transfected into cells using FuGENE® HD transfection reagent (Roche Diagnostics GmbH) at 37˚C for 48 h, according to the manufacturer's protocol. After 48 h of transfection, transfection efficiencies were determined using reverse transcription-quantitative PCR (RT-qPCR).

Cell Counting Kit-8 (CCK-8) assay. A CCK-8 assay (Dojindo Molecular Technologies, Inc.) was used to study cell viability. A total of $2x10^3$ cells/well were plated in 96-well plates and cultured for 24, 48, 72 and 96 h at 37˚C. Subsequently, 10 μl CCK-8 solution was added to each well and incubated with the cells at 37˚C with 5% CO_2 for 4 h. The absorbance was measured at a wavelength of 450 nm.

Wound healing assay. Cells were cultured for 24 h until the cell confluence reached ~90%. A scratch was then made in the cell monolayer using a pipette tip to create an artificial wound. The cells were washed twice with PBS and incubated with serum-free DMEM at 37˚C. The cells were visualized in the same position after 0, 24 and 48 h to determine the migratory distance. Images were obtained under a light microscope. Wound healing was calculated according to the following formula: Relative wound healing (%)=(0 h scratch distance-24/48 h scratch distance)/0 h scratch distance x100.

Transwell assays. The Transwell assays were performed as described by Li *et al* (21). Briefly, the cells were cultured in serum-free DMEM, then trypsinized. The cell density was adjusted to $1x10^6$ cells/ml, and cells were seeded into the upper chamber of a 24-well Transwell culture plate. DMEM supplemented with 10% FBS was added to the lower chamber

of the Transwell plate. The cells were then incubated for 24 h for evaluation of migration. After 24 h, the cells on the surface of the lower chamber membrane were fixed with 5% glutaraldehyde for 15 min at room temperature and then stained with 0.1% crystal violet for 20 min at room temperature. Stained cells were visualized using a light microscope in three randomly selected fields of view. To evaluate the invasive ability of cells, 200 μl cells (1x10^6 cells/ml) were seeded into the upper chambers of Transwell plates with 50 mg/l Matrigel (8 μm; cat. no. CLS3374; Corning, Inc.) and serum-free medium after Matrigel precoating at 37˚C for 1 h. 500 μl DMEM supplemented with 10% FBS was added to the lower chamber. Following incubation at 37˚C for 24 h, the cells remaining in the upper chamber were removed, whereas cells in the lower chamber were fixed with 5% glutaraldehyde for 15 min at 4˚C, washed with PBS and stained with 0.1% crystal violet (Sigma-Aldrich; Merck KGaA) for 20 min at room temperature. Stained cells were visualized using a light microscope in three randomly selected fields of view.

Colony formation assay. After 24 h of transfection, cells were digested with 0.25% trypsin to prepare a single cell suspension. The cells were then seeded into a 6-well culture plate at a density of 500 cells/well (three repeats/experimental group) and cultured at 37˚C in a 5% CO_2 incubator. The culture medium was changed every 3 days during the culture period. After 15 days, the culture was terminated upon the appearance of visible colonies in the culture dish. The medium was subsequently discarded, the cells were washed with pre-cooled (4˚C) PBS 2-3 times, and then fixed with 5 ml pure methanol for 15 min at room temperature. The cells were washed another three times with PBS and subsequently stained with Giemsa staining solution for 15 min at room temperature. Stained cells were visualized using a light microscope (magnification, x5) to count the number of colonies with >10 cells.

RNA pull-down assay. Biotinylated miR-25-5p probe (5'-AGG CGGAGACUUGGGCAAUUG-Biotin-3') and control probe (5'-GTTAACGGGTTCAGAGGCGGA-Biotin-3') were synthesized by Sangon Biotech Co., Ltd. First, cells (1x10^7) were lysed with 500 μl RIP lysis buffer centrifuged at 4˚C and 12,000 x g for 15 min, and the cell lysate in the supernatant was collected. The Pierce Magnetic RNA-Protein Pull-Down kit (Thermo Fisher Scientific, Inc.) was used for RNA pull-down experiments. Biotinylated RNA probes (miR-25-5p probe and control probe) and 400 μl streptavidin magnetic beads (Thermo Fisher Scientific, Inc.) were incubated with cell lysates overnight at 4˚C. After proteinase K digestion at 55˚C for 20 min, the RNA attached to the magnetic beads was separated twice with washing buffer, and then centrifuged at 5,000 x g for 30 sec at 4˚C to collect the Bio-miR/mRNA mixture, after which RT-qPCR was performed.

Dual-luciferase reporter assay. TargetScan (targetscan.org/vert_72/) and miRanda (microrna.org/microrna/home.do) databases were used to predict the target genes of miR-25. The reporter vector pmirGLO-DKK3-wild-type (wt), pmirGLO-DKK3-mutant (mut), pmirGLO-MICAL2-1-wt and pmirGLO-MICAL2-1-mut plasmids, or synthetic miR-NC mimics (forward, 5'-UUGUACUACACAAAAGUACUG-3' and reverse, 5'-GUACUUUUGUGUAGUACAAUU-3') or miR-25 mimics (forward, 5'-AGGCGGAGACUUGGG CAAUUG-3' and reverse, 5'-AUUGCCCAAGUCUCCGCC UUU-3') were obtained from Sangon Biotech Co., Ltd. Upon cell confluence reaching 70-80%, each reporter plasmid was co-transfected into 293T cells alongside miR-NC mimics or miR-25 mimics using Lipofectamine® 2000 (Invitrogen; Thermo Fisher Scientific, Inc.). A total of 24 h after transfection, the relative firefly luciferase activity was detected using a Dual-Glo Luciferase Reporter assay system, according to the manufacturer's protocol (Promega Corporation). The relative luciferase activity was normalized to *Renilla* luciferase activity.

Fluorescence colocalization analysis. Cells transfected with the lnc-MICAL2-1 overexpression or control NC vector for 48 h, or transfected with lnc-MICAL2-1 knockdown or control NC vector were washed with PBS once and fixed with methanol for 15 min at room temperature. Subsequently, cells were incubated with an anti-β-catenin primary antibody (1:500; cat. no. ab32572; Abcam) overnight at 4˚C. After primary antibody incubation, the cells were incubated with a TRITC-conjugated goat anti-rabbit IgG antibody (cat. no. TA130015 1:200; OriGene Technologies, Inc.) for 1 h at room temperature. The nuclei were counterstained with DAPI for 5 min at room temperature. Stained cells were visualized using a fluorescence microscope.

Cell cycle analysis. After 72 h of transfection, cells were trypsinized and 2x10^5 cells/ml were plated in a 6-well culture plate. The cells were fixed with 75% ice-cold ethanol at 4˚C for at least 30 min, then washed with PBS to remove the fixative solution. Following the addition of 100 μl RNase, the cells were incubated in a water bath at 37˚C for 30 min. Cells were subsequently incubated with 400 μl propidium iodide (PI; Sigma-Aldrich; Merck KGaA) at 4˚C in the dark for 30 min. A ACEA NovoCyte flow cytometer (ACEA Bioscience, Inc.) with NovoExpress Software (version 1.0.2; ACEA Biosciences, Inc.) was used for cell cycle distribution analysis.

Flow cytometry analysis of apoptosis. Cells in the logarithmic growth phase were collected and seeded into a 6-well plate at a density of 1x10^5 cells/well, then incubated with 5% CO_2 at 37˚C for 18 h. Cells were then transfected with lnc-MICAL2-1 overexpression, knockdown or NC vectors. After 48 h, 1-5x10^5 cells were harvested and resuspended in 1X PBS. A total of 5 μl Annexin V-FITC and 5 μl PI was added and incubated at room temperature for 5 min in the dark. Apoptotic cells were analyzed using a flow cytometer (FACSCalibur; BD Biosciences) with BD Cell Quest Pro Software (version 3.3; Becton, Dickinson and Company).

RT-qPCR. Total RNA was extracted from cells using TRIzol® reagent (Invitrogen; Thermo Fisher Scientific, Inc.). The purity of total RNA was detected and quantified using an UV spectrophotometer (260 nm to calculate RNA concentration and 260/280 nm to evaluate RNA purity). Then, total RNA (1 μg) was reverse transcribed into cDNA using a reverse transcription system (cat. no. A3500; Promega Corporation), according to the manufacturer's protocol. Primer3web software (version 4.1.0;

http://primer3.ut.ee/) was used to design the following primers for qPCR: GAPDH (NM_001256799.3) forward, 5'-GAAAGC CTGCCGGTGACTAA-3' and reverse, 5'-TTCCCGTTCTCA GCCTTGAC-3'; DKK3 (NM_001018057.2) forward, 5'-CCT GGCAAACTTACCTCCCA-3' and reverse, 5'-CATTTTGGT GCAGTGACCCC-3'; lnc-MICAL2-1 forward, 5'-TCAGCC TGCCTGCCAATATG-3' and reverse, 5'-AAGCAGTGC TGCAAGGAAGA-3'; miR-25-5p forward, 5'-AGGCGGAGA CTTGGGCAATTG-3' and reverse, 5'-GTGCGTGTCGTG GAGTCG-3'; and U6 forward, 5'-CTCGCTTCGGCAGCA CACAATTG-3' and reverse, 5'-AACGCTTCACGAATT TGCGT-3'. qPCR was performed on an ABI 7500 Real-Time PCR Detection system (Applied Biosystems; Thermo Fisher Scientific, Inc.). The thermocycling conditions were as follows: Initial denaturation at 95˚C for 10 min; 40 cycles of denaturation at 95˚C for 10 sec, annealing and extension at 60˚C for 1 min. mRNA and miRNA expression levels were determined using the $2^{-\Delta\Delta Cq}$ method (22). GAPDH was used as the mRNA housekeeping gene and U6 was used as the miRNA housekeeping gene.

Western blotting. Total protein was extracted from cells using RIPA lysis buffer (Beyotime Institute of Biotechnology). Total protein was quantified using a BCA protein assay kit (Bio-Rad Laboratories, Inc.), loaded on a 12% SDS gel and resolved using 10% SDS-PAGE (NuPAGE; Invitrogen; Thermo Fisher Scientific, Inc.). The separated proteins were subsequently transferred to PVDF membranes (Whatman plc; Cytiva) and blocked with 5% non-fat dry milk powder (Merck KGaA) at room temperature for 2 h. The PVDF membrane was then incubated with DKK3 (1:1,000; cat. no. ab187532; Abcam) primary antibodies at 4˚C overnight. After the primary antibody incubation, the membranes were washed with TBS-Tween 20 (0.05%) three times and incubated with a goat anti-rabbit secondary antibody (cat. no. bs-0295G-HRP; 1:3,000; BIOSS) for 2 h at room temperature. Protein bands were visualized using chemiluminescence reagent on a gel imaging system (Thermo Fisher Scientific, Inc.). The band densities were analyzed using ImageJ software (version 4.6; National Institutes of Health). The gray value of the target protein was normalized to the gray value of the internal reference protein, GAPDH, and the data are presented as the relative content of the target protein in a sample.

Establishment of a xenograft model. A total of 63 male BALB/c-nude mice (5-week-old; weight 18-20 g; Chengdu Dashuo Laboratory Animal Co., Ltd.) were maintained in aseptic conditions at 25˚C and 40-60% humidity, with 12-h light/dark cycles, and free access to food and water. Mice were subcutaneously injected with $1x10^7$ MCF-7 cells stably transfected with lnc-MICAL2-1 overexpression, knockdown or NC. After inoculation, the tumor volume was measured once a week. After 6 weeks, the mice (n=6 per group) were euthanized via cervical dislocation, the tumor tissue was harvested, and the weight and volume were measured. The volume of the tumor was calculated using the following equation: Volume=length x $width^2$ x0.5, where the length represented the longest diameter and the width represented the shortest diameter of the tumor. The maximum tumor diameter observed in the present study was 1.84 cm and the maximum tumor volume was 1,935.3 mm^3. To evaluate the survival of mice, 15 mice from each group were observed until the 10th week. If ulceration, infection or necrosis occurred, or mice were on the verge of death, the experiment was terminated and the mice were euthanized. The survival rate of tumor-bearing mice after inoculation with tumor cells was analyzed using the Kaplan-Meier method. The log-rank (Mantel-Cox) test was used to determine statistical differences in the survival curves. All animal procedures and experimental methods were approved by the Committee on the Ethics of Animal Experiments of Southern Medical University (approval no. SYXK 2020-0012). This study was performed in strict accordance with the recommendations in the Guide for the Care and Use of Laboratory Animals of the National Institutes of Health (23), and in accordance with the Animal Research: Reporting *In Vivo* Experiments guidelines (24).

Hematoxylin and eosin (H&E) staining. Tumor tissues were fixed with 4% neutral formaldehyde for 24 h at room temperature, routinely embedded in paraffin and cut into 4-μm slices. After conventional dewaxing, the sections were stained with hematoxylin at room temperature for 5 min and eosin for 3 min at room temperature. Then, graded alcohol dehydration, xylene clearing and neutral gum sealing were performed. The morphological changes of tumor cells were observed under a light microscope.

Immunohistochemistry. Tumor tissues were embedded in paraffin, sectioned into 5-μm slices, heated for 2 h at 60˚C, Subsequently, the tissues were deparaffinized with xylene I and II (each for 10 min), and dehydrated in a gradient alcohol series. Heat-mediated antigen retrieval was performed with citrate buffer (pH 6), then the sections were immersed in 3% hydrogen peroxide for 10 min to block endogenous peroxidase, followed by blocking with 5% bovine serum albumin (Wuhan Servicebio Technology Co., Ltd.) for 30 min at room temperature. The sections were subsequently incubated with 50 μl anti-DKK3 rabbit monoclonal antibody (1:100; cat. no. ab187532; Abcam), MMP-25 (1:100; cat. no. ab56309; Abcam) overnight at 4˚C. Following the primary antibody incubation, the sections were washed with PBS for 2 min and incubated with 50 μl biotinylated goat anti-rabbit IgG (1:100; cat. no. bs-0295G-HRP; BIOSS) at 37˚C for 30 min. Sections were then washed with PBS three times (15 min each), and then incubated with high sensitivity streptavidin-HRP conjugate (Biosynthesis Biotechnology Co., Ltd.) for 30 min at 37˚C. Sections were stained with DAB (Biosynthesis Biotechnology Co., Ltd.) for 8 min at room temperature and hematoxylin for 5 min at room temperature, then dehydrated in gradient ethanol for 1 min, made transparent with xylene and sealed with neutral gum. The immunostaining images were captured using a light microscope (magnification, x400). The integrated optical density in the selected area was calculated in five non-overlapping fields of view of each section as the statistical area. Image-Pro Plus 6.0 software (Media Cybernetics, Inc.) was used for the analysis.

Statistical analysis. Statistical analysis was performed using GraphPad Prism 5.0 software (GraphPad Software, Inc.). Statistical differences between two groups were compared using the non-parametric Mann Whitney-U test, whereas a Kruskal-Wallis test and Dunn's post hoc test was used for the

comparisons between more than two groups. The differential expression of lncRNAs was analyzed using an unpaired Student's t-test between tumor and adjacent normal tissues. Spearman's rank correlation analysis was used to determine the correlation between lncRNA and mRNA expression. The nonparametric Kaplan-Meier method was used for survival analysis. The log-rank (Mantel-Cox) test was used to compare the difference between survival curves. $P<0.05$ was considered to indicate a statistically significant difference.

Results

Expression levels of lnc-MICAL2-1 in BC, and association with DKK3 expression and clinicopathological parameters. To determine the underlying mechanism of downregulated DKK3 expression in BC, the GeneCards bioinformatics tool was used. The results revealed that lnc-MICAL2-1 may regulate DKK3 expression via modulation of miR-25. The expression levels of lnc-MICAL2-1 in the tumor tissues of patients with breast invasive carcinoma (BRCA) obtained from TCGA database were analyzed. The results demonstrated that the expression levels of lnc-MICAL2-1 were downregulated in human BRCA tissues compared with those in normal tissues The results also found that the expression levels of lnc-MICAL2-1 were significantly downregulated in tumor tissues (n=837) compared with in adjacent normal tissues (n=105) (Fig. 1A). Breast cancer is divided according to the expression matrix by molecular profiling (GEP). For example, PAM50-based GEP can divide breast cancer into different subtypes, including normal-like, basal, luminal A, luminal B and Her2. Analysis of lnc-MICAL2-1 expression in the PAM50 subtype of BRCA samples identified significant differences between the basal and luminal A subtypes (Fig. 1B). Correlation analysis in basal, luminal B and human epidermal growth factor receptor 2 (Her2) subtypes of BC identified a positive correlation between lnc-MICAL2-1 and DKK3 mRNA expression in the basal (correlation, 0.3569581; $P<0.05$; n=139), luminal B (correlation, 0.4869612; $P<0.05$; n=191) and Her2 (correlation, 0.4401873; $P<0.05$; n=67) subtypes (Fig. 1C-E). According to the median expression of lnc-MICAL2-1 in all patients, the patients were divided into high expression and low expression groups. Survival analysis showed that high expression levels of lnc-MICAL2-1 decreased the overall survival rate of BC and was thus indicative of a poorer prognosis (Fig. 1F). The association between the expression of lnc-MICAL2-1 and the estrogen receptor, progesterone receptor and therapy of patients with BC was statistically significant ($P<0.05$), but there was no association with staging and HER2 expression ($P>0.05$) (Fig. 1G-K).

Effects of the knockdown and overexpression of lnc-MICAL2-1 on BC cell proliferation, invasion and migration. To further understand the effects of lnc-MICAL2-1 on BC cells, lnc-MICAL2-1 overexpression and knockdown vectors were constructed and transfected into the BC cell lines, MCF-7 and MBA-MD-231 (Fig. 2A and B). The results revealed that the optical density value was decreased following the overexpression of lnc-MICAL2-1 in BC cells, suggesting that cell proliferation was inhibited. Conversely, the proliferative ability of cells with lnc-MICAL2-1 knockdown was significantly increased (Fig. 2C and D). In addition, a wound healing assay was performed using transfected MCF-7 cells to determine the effects on cell migration (Fig. 2E). The results demonstrated that cell migration was inhibited following the overexpression of lnc-MICAL2-1, whereas the knockdown of lnc-MICAL2-1 promoted cell migration (Fig. 2F). The results of the Transwell assays indicated that the overexpression of lnc-MICAL2-1 inhibited the invasive and migratory ability of MCF-7 cells (Fig. 2G-J). The data from the colony formation assay experiments further validated that the overexpression of lnc-MICAL2-1 inhibited cell proliferation (Fig. 2K and L).

lnc-MICAL2-1 upregulates DKK3 expression via sponging miR-25. A positive correlation was identified between lnc-MICAL2-1 and DKK3 mRNA expression in BC tissues (correlation, 0.632; n=47; $P<0.05$; Fig. 3A). Subsequently, lnc-MICAL2-1 was overexpressed or knocked down in MCF-7 and MDA-MB-231 cells. The results revealed that in MCF-7 cells overexpressing lnc-MICAL2-1, the mRNA and protein expression levels of DKK3 were significantly upregulated. Conversely, following the knockdown of lnc-MICAL2-1 expression in MCF-7 cells, the mRNA and protein expression levels of DKK3 were significantly downregulated (Fig. 3B-D). Therefore, it was hypothesized that lnc-MICAL2-1 may exert a positive regulatory effect on DKK3 expression. Bioinformatics analysis identified 13 complementary base pairings between miR-25 and lnc-MICAL2-1 (Fig. 3E). Similarly, complementary base pairings were identified between miR-25 and DKK3 (Fig. 3F). A previous study reported that miR-25 targeted DKK3 and regulated the Wnt/β-catenin signaling pathway (12). Therefore, dual-luciferase reporter and RNA pull-down assays were performed to validate the binding. The results of dual-luciferase reporter showed that compared with miRNA NC, the luciferase activity in wt-lnc-MICAL2-1 cells transfected with miRNA-25 mimic was significantly decreased ($P<0.01$), whereas the luciferase activity in mut-lnc-MICAL2-1 cells was not affected ($P>0.05$) (Fig. 3G). The results revealed that lnc-MICAL2-1 was able to sponge miR-25. This relationship was further determined using the RNA pull-down assay. The results indicated that lnc-MICAL2-1 could be pulled down by miRNA-25 (Fig. 3H). The results of the dual-luciferase reporter assay showed that compared with the miRNA NC group, the luciferase activity in wt-DKK3 cells transfected with miRNA-25 mimic was significantly decreased ($P<0.01$), but the luciferase activity in mut-DKK3 cells was not affected ($P>0.05$) (Fig. 3I). This relationship was further determined using the RNA pull-down assay, whereby DKK3 was pulled down by miRNA-25 (Fig. 3J). These findings suggested that lnc-MICAL2-1 may have reduced the degradation of DKK3 mRNA by sponging miR-25, thereby exerting an indirect positive regulatory effect on DKK3.

lnc-MICAL2-1 upregulates DKK3 expression and downregulates the Wnt signaling pathway. To explore the regulatory effect of lnc-MICAL2-1 on the DKK3-mediated Wnt signaling pathway, a lnc-MICAL2-1 overexpression plasmid and miR-25 mimic were co-transfected into MCF-7 cells, and shRNA lnc-MICAL2-1 and miR-25 inhibitor were co-transfected into MCF-7 cells. Transfection efficiency of miR-25 mimic and inhibitor were determined by RT-qPCR

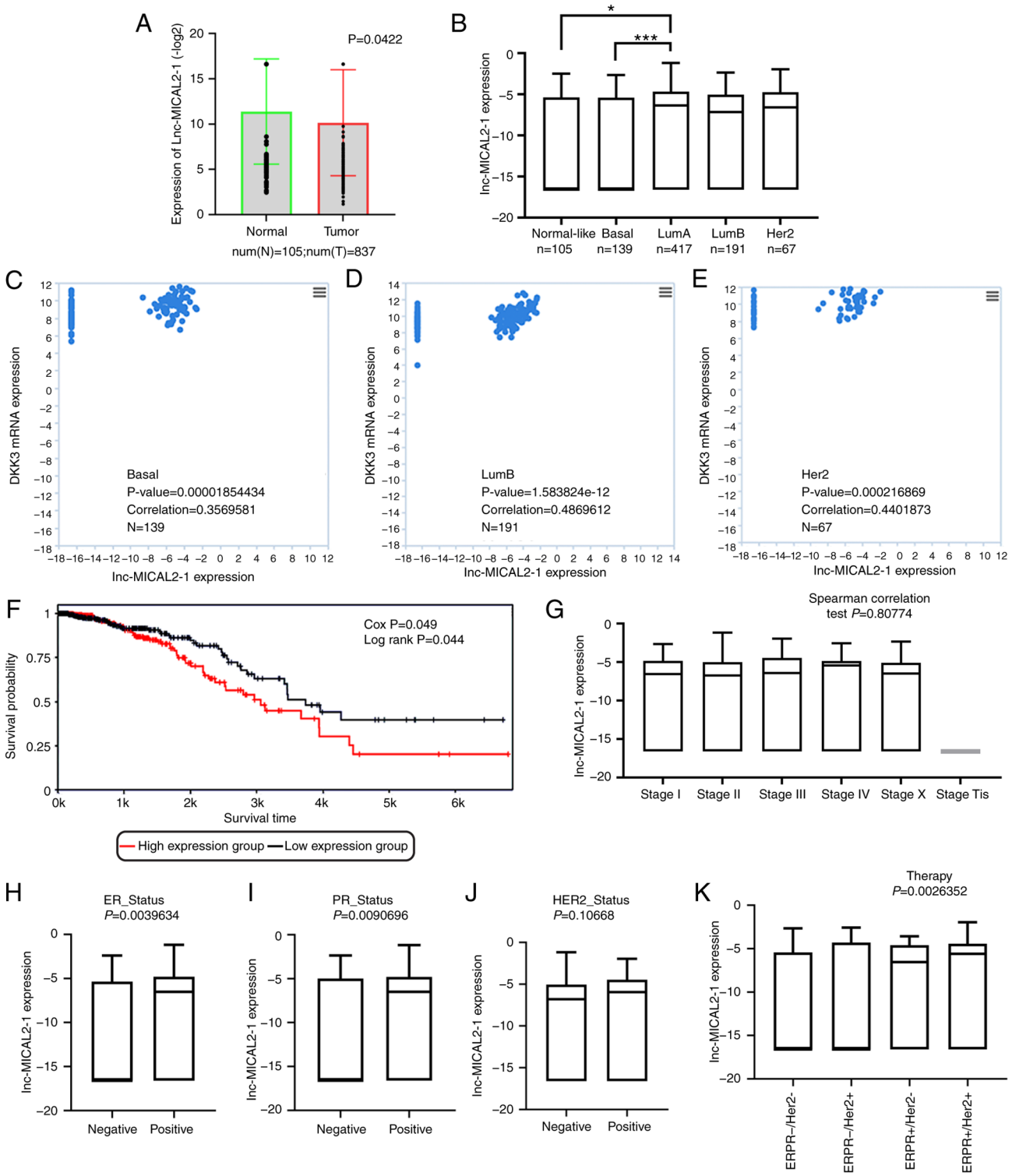

Figure 1. lnc-MICAL2-1 expression is downregulated in BC and is associated with DKK3 expression. (A) TANRIC database analysis of the expression of lnc-MICAL2-1 in BC tissues: Normal tissues, n=105; tumor tissues, n=837. P<0.05. (B) Expression of lnc-MICAL2-1 in the PAM50 subtype of BC. TANRIC database analysis of the association between the expression of lnc-MICAL2-1 and DKK3 mRNA in (C) basal, (D) LumB and (E) Her2 subtypes of breast invasive carcinoma. P<0.05. (F) Relationship between the expression levels of lnc-MICAL2-1 and the overall survival rate of patients with BC. TANRIC database analysis of the association between the expression of lnc-MICAL2-1 and (G) staging, (H) ER, (I) PR, (J) HER2 and (K) therapy. *P<0.05, ***P<0.001. Num, Number; Lum A, luminal A; Lum B, luminal B; DKK3, Dickkopf 3; ER, estrogen receptor; PR, progesterone receptor; HER2, human epidermal growth factor receptor 2; lnc-MICAL2-1, long non-coding RNA MICAL2-1; BC/BRCA, breast cancer; TANRIC, The Atlas of ncRNA in Cancer.

in MCF-7 cells, and the results showed that the transfection was successful (Fig. 4A). Furthermore, the results revealed that the mRNA and protein expression levels of DKK3 in cells co-transfected with the lnc-MICAL2-1 overexpression vector and miR-25 mimic were downregulated compared with in cells only transfected with the lnc-MICAL2-1 overexpression vector (Fig. 4B-D). Conversely, the mRNA and protein expression levels of DKK3 in cells co-transfected

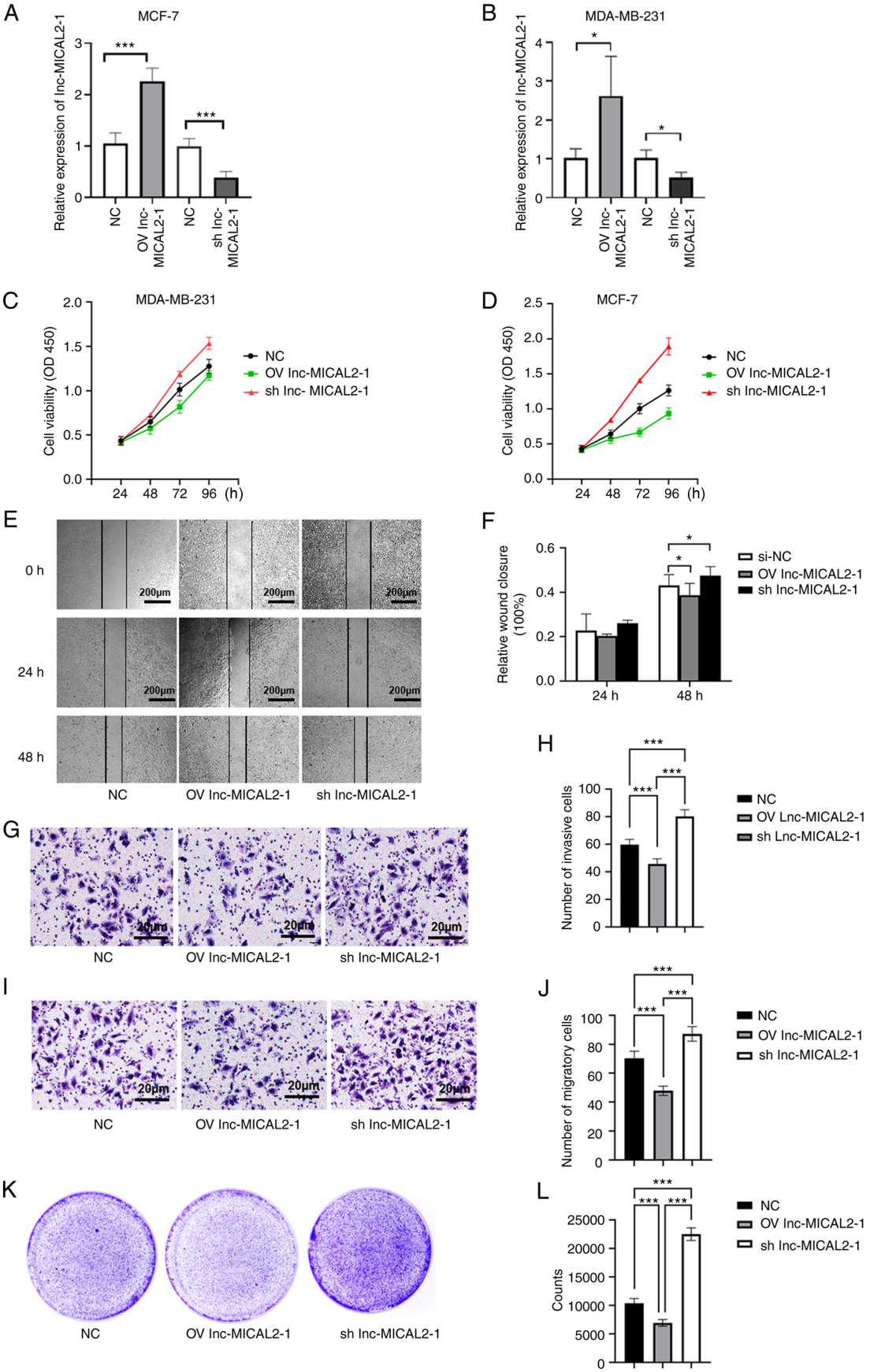

Figure 2. lnc-MICAL2-1 inhibits breast cancer cell proliferation, migration and invasion. (A and B) Reverse transcription-quantitative PCR was used to determine the transfection efficiency of lnc-MICAL2-1 overexpression or knockdown. The viability of (C) MBA-MB-231 cells and (D) MCF-7 cells was detected using a Cell Counting Kit-8 assay. (E and F) Migration of MCF-7 cells was detected using a wound-healing assay. (G and H) Invasion and (I and J) migration of MCF-7 cells were assessed using Transwell assays. (K and L) Proliferation of MCF-7 cells was detected using a colony formation assay (magnification, x5). Data are presented as the mean ± standard deviation. *P<0.05, ***P<0.001. NC, negative control; lnc-MICAL2-1, long non-coding RNA MICAL2-1; OV, overexpression; sh, short hairpin.

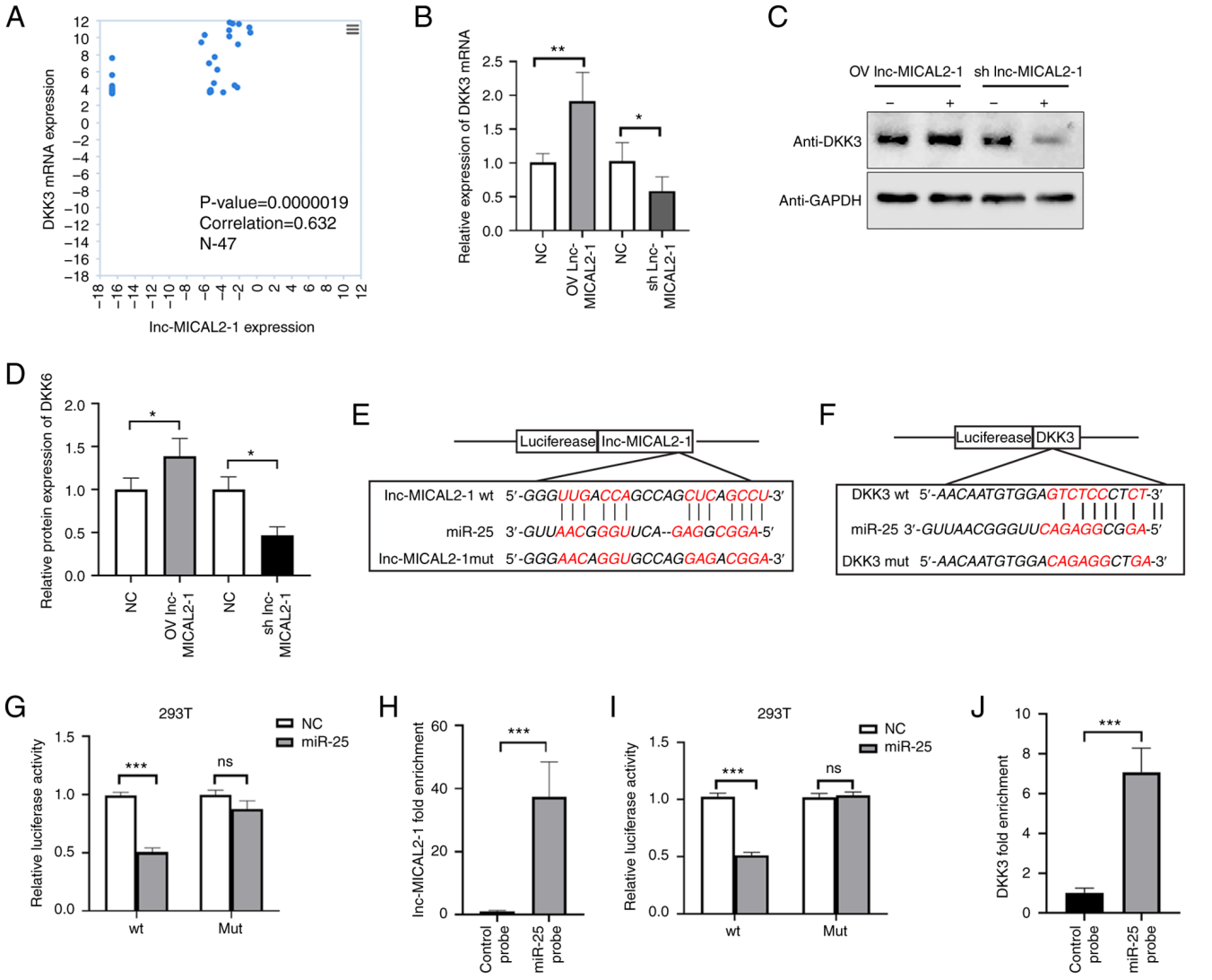

Figure 3. lnc-MICAL2-1 sponges miR-25 as a competing endogenous RNA, indirectly enhancing DKK3 gene transcription. (A) Analysis of data obtained from The Atlas of non-coding RNA in Cancer, assessing the relationship between lnc-MICAL2-1 and DKK3 expression in breast cancer. (B) Reverse transcription-quantitative PCR was used to determine the effect of lnc-MICAL2-1 OV or knockdown on DKK3 mRNA expression. (C and D) Western blotting was used to assess the effect of lnc-MICAL2-1 OV or knockdown on DKK3 expression levels. The predicted binding sites between (E) miR-25 and lnc-MICAL2-1, and (F) miR-25 and DKK3. (G) The target relationship between lnc-MICAL2-1 and miR-25 was verified using a dual-luciferase reporter assay. (H) RNA pull-down assay detected the molecular interaction between lnc-MICAL2-1 and miR-25. (I) The target relationship between DKK3 and miR-25 was verified by dual-luciferase reporter assay. (J) An RNA pull-down assay detected the molecular interaction between DKK3 and miR-25. Data are presented as the mean ± standard deviation. *P<0.05, **P<0.01, ***P<0.001. DKK3, Dickkopf 3; lnc-MICAL2-1, long non-coding RNA MICAL2-1; OV, overexpression; miR, microRNA; WT, wild-type; MUT, mutant; sh, short hairpin.

with shRNA lnc-MICAL2-1 and miR-25 inhibitor were upregulated compared with in cells transfected with shRNA lnc-MICAL2-1 only (Fig. 4E-G). In addition, the overexpression of lnc-MICAL2-1 decreased β-catenin nuclear localization, whereas shRNA lnc-MICAL2-1 increased the translocation of β-catenin into the nucleus (Fig. 4H). Next, the effect of lnc-MICAL2-1 on the β-catenin signaling pathway-mediated apoptosis of MCF-7 cells was explored. Activation of the Wnt/β-catenin pathway affects cell apoptosis and cell cycle progression (25). The data revealed that in the lnc-MICAL2-1 knockdown cells, the number of cells in the S phase of the cell cycle was significantly increased compared with that in the control cells (Fig. 4I and J), whereas the levels of apoptosis were significantly increased following the overexpression of lnc-MICAL2-1 in MCF-7 cells compared with in the control cells (Fig. 4K and L).

lnc-MICAL2-1 inhibits tumor growth in vivo via regulation of the Wnt signaling pathway. To further explore the inhibitory function of lnc-MICAL2-1 on BC cells, a BC xenograft model was established. The overexpression of lnc-MICAL2-1 significantly reduced tumor weight (Fig. 5A) and volume (Fig. 5B) compared with in the control and lnc-MICAL2-1 knockdown groups. The survival curve also revealed that the overexpression of lnc-MICAL2-1 significantly prolonged the survival time of mice compared with in the control group (Fig. 5C).

H&E staining showed that NC group tumors grew rapidly with a different morphology. Inflammatory infiltration was observed around the edges of the tumor tissues, as well as a small number of necrotizing cells. The tumors in the lnc-MICAL2-1 group displayed a reduced number of tumor cells, increased cell degeneration and necrosis,

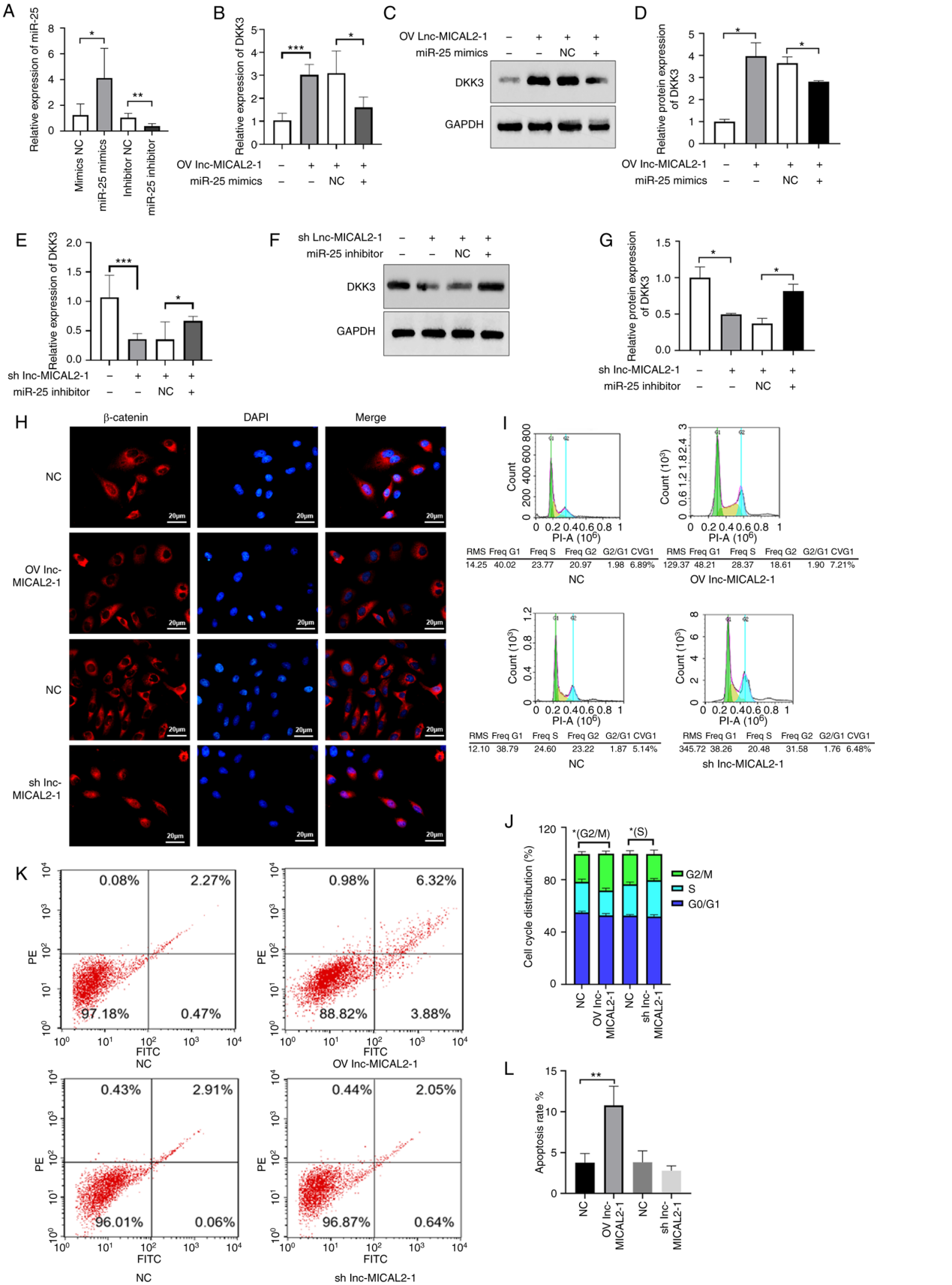

Figure 4. lnc-MICAL2-1 enhances DKK3 gene transcription and downregulates the Wnt signaling pathway. (A) Transfection efficiency of miR-25 mimic and inhibitor determined by reverse transcription-quantitative PCR in MCF-7 cells. Overexpression of lnc-MICAL2-1 competitively binds and absorbs miR-25, increasing DKK3 (B) mRNA and (C and D) protein expression levels. Knockdown of lnc-MICAL2-1 results in increased miR-25 levels, thus reducing DKK3 (E) mRNA and (F and G) protein expression. (H) Immunofluorescence staining of β-catenin and DAPI staining of the nuclei. (I and J) Cell cycle distribution analysis was performed to determine the effect of overexpression or knockdown of lnc-MICAL2-1 on cell cycle progression. (K and L) Flow cytometric analysis of the effect of OV or knockdown of lnc-MICAL2-1 on cell apoptosis. Data are presented as the mean ± standard deviation. *P<0.05, **P<0.01, ***P<0.001. DKK3, Dickkopf 3; OV, overexpression; miR, microRNA; sh, short hairpin; NC, negative control; lnc-MICAL2-1, long non-coding RNA MICAL2-1.

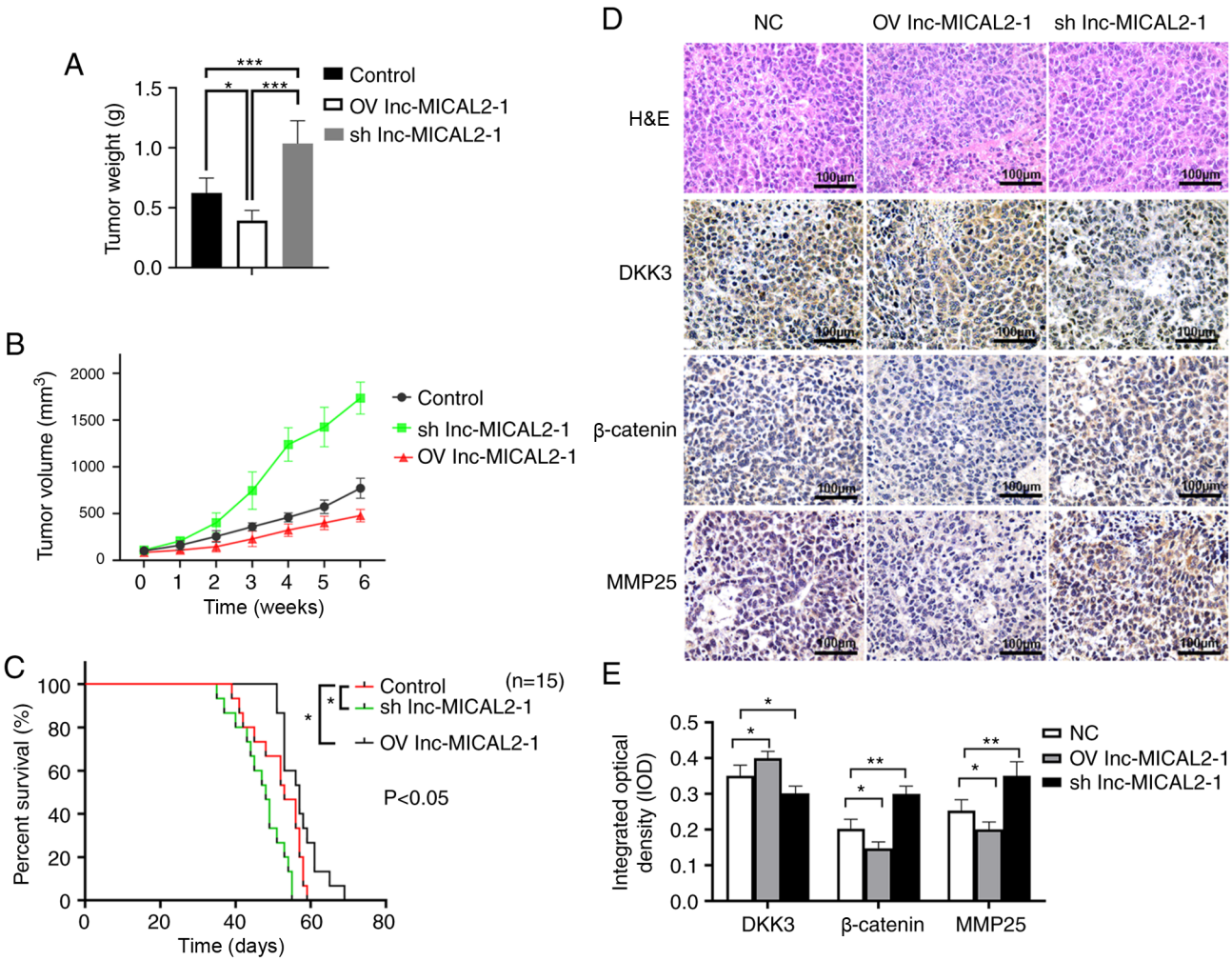

Figure 5. lnc-MICAL2-1 inhibits the tumor growth *in vivo* via regulation of the Wnt signaling pathway. (A) Tumor weight and (B) tumor volume in a xenograft mouse model of breast cancer established using MCF-7 cells. n=6. (C) Effect of lnc-MICAL2-1 on survival *in vivo*. n=15. (D and E) H&E staining and the expression of DKK3, β-catenin and MMP25 detected using immunohistochemistry. Data are presented as the mean ± standard deviation. *P<0.05, **P<0.01, ***P<0.001. OV, overexpression; sh, short hairpin; NC, negative control; H&E, hematoxylin and eosin; DKK3, Dickkopf 3; MMP25, matrix metalloproteinase 25.

and an enhanced tissue response (Fig. 5D). The results of immunohistochemistry showed that the knockdown of lnc-MICAL2-1 downregulated the expression levels of DKK3, whereas the expression levels of β-catenin and MMP-25 were upregulated (Fig. 5D and E). These findings suggested that lnc-MICAL2-1 expression may be positively associated with DKK3 expression, whereas DKK3 expression may be negatively associated with the expression of β-catenin and MMP-25 (Fig. 5D and E).

Discussion

DKK3 is a tumor suppressor gene and its expression has been reported to be downregulated in numerous types of cancer, including prostate (26), gastric (27), pancreatic (28), lung and renal cell (29) cancer. A previous study reported that DKK3 could inhibit the Wnt signaling pathway by blocking planar cell polarity (30). However, the upstream regulatory mechanism of DKK3 in BC requires further investigation.

lncRNAs are known to act as ceRNAs (endogenous sponges) to downregulate miRNA expression and thereby reduce the translational inhibition of miRNA target genes (18). The abnormal expression of lncRNAs has been discovered to play an important role in the progression of cancer, including BC (21). It has been shown that lncRNA MEG3 can regulate E-cadherin expression by adsorbing miR-421 in BC cells (31). lncRNA HOTAIR has also been reported to regulate HMGA2 through sponging miR-20a-5p to affect BC cell proliferation, migration, invasion and apoptosis (32). However, the upstream lncRNA involved in the regulation of DKK3 was unknown, to the best of our knowledge.

The present study first predicted the upstream regulatory miRNA and lncRNA of DKK3 through bioinformatics analysis. The results demonstrated that lnc-MICAL2-1 upregulated the expression levels of DKK3 in invasive BRCA, suggesting a positive association between lnc-MICAL2-1 and DKK3. The expression levels of lnc-MICAL2-1 had a positive relationship with the clinical characteristics and overall survival rate of patients with BC. In order to confirm the effect of lnc-MICAL2-1 on BC cells, lnc-MICAL2-1 knockdown and overexpression vectors were transfected into BC cells, and cellular behavior experiments were performed. The results showed that lnc-MICAL2-1 inhibited BC cell proliferation, migration and invasion. Previous studies have

shown that the expression levels of miR-25 were significantly upregulated in human tumor tissues and cells, such as melanoma, glioma and non-small cell lung cancer, which promoted cell invasion and proliferation by targeting DKK3 (11,12). However, the targeting relationship between lnc-MICAL2-1 and miR-25 is unclear. Using the GeneCards database, it was further predicted that lnc-MICAL2-1 and miR-25, as well as miR-25 and DKK3 possess complementary binding sites with each other, respectively. To further understand the relationship between lnc-MICAL2-1, miR-25 and DKK3, bioinformatics analysis was used to determine the binding site between lnc-MICAL2-1 and miR-25, then dual-luciferase reporter and RNA pull-down assays were used to validate the competitive binding relationship between lnc-MICAL2-1 and miR-25. The results of the dual luciferase reporter assay and RNA pull-down assays further confirmed that DKK3 was a target gene of miR-25.

DKK3 is an antagonist of the Wnt signaling pathway. The inactivation of DKK3 has been shown to be related to the poor prognosis of various solid tumors and hematological malignancies (12). The Wnt signaling pathway is a conserved and complex signaling pathway, which regulates stem cell self-renewal, cell proliferation, differentiation and apoptosis, and participates in embryonic development, tissue homeostasis and carcinogenesis (33,34). DKK3 was discovered to bind to the Wnt-signaling member LDL receptor-related 5/6 or kringle containing transmembrane protein 1/2 to negatively regulate the Wnt signaling pathway (35). The activation of the Wnt signaling pathway causes a reduction in β-catenin degradation and the accumulation of β-catenin in the cytoplasm. β-catenin can enter the nucleus to form complexes, affecting the proliferation, cell cycle and apoptosis of tumor cells, amongst other behaviors (36). To further understand the involvement of lnc-MICAL2-1 in the downstream signaling cascade, the localization of β-catenin in BC cells was analyzed. Overexpression of lnc-MICAL2-1 decreased β-catenin nuclear localization, whereas shRNA lnc-MICAL2-1 increased the nuclear translocation of β-catenin, suggesting that lnc-MICAL2-1 downregulated the Wnt signaling pathway. The results of the present study also discovered that the knockdown of lnc-MICAL2-1 increased the number of cells in the S phase of the cell cycle and

To further explore the inhibitory effect of lnc-MICAL2-1 on BC cells, a BC xenograft model was established. The results revealed that the knockdown of lnc-MICAL2-1 downregulated the expression levels of DKK3, whereas the expression levels of β-catenin were upregulated.

In conclusion, the present study discovered that lnc-MICAL2-1 may be a good prognostic marker, since it may act as a tumor suppressor in BC. lnc-MICAL2-1, as a ceRNA, was demonstrated to sponge miR-25 and further stabilize DKK3, thereby reducing Wnt/β-catenin signaling pathway activation. These findings uncovered novel potential targets for BC, which provides a new research direction for molecular targeted therapy and further investigations into the underlying pathogenesis of BC.

Acknowledgements

Not applicable.

Funding

The present study was supported by the Natural Science Foundation of Hainan Province (grant no. 818QN3143).

Availability of data and materials

All data generated or analyzed during the present study are available from the corresponding author on reasonable request.

Authors' contributions

JY, GL, ML and SY conceived and designed the study. HS performed the experiments. JY, GL, ML and CY performed the data analysis. JY, GL and ML wrote the manuscript. JY and SY confirm the authenticity of all the raw data. All authors edited the manuscript. All authors have read and approved the manuscript.

Ethics approval and consent to participate

The animal experiments performed in the present study were approved by the Committee on the Ethics of Animal Experiments of Southern Medical University (approval no. SYXK 2020-0012). The authors declare that this study was performed in strict accordance with the recommendations in the Guide for the Care and Use of Laboratory Animals of the National Institutes of Health, and in accordance with the Animal Research: Reporting *In Vivo* Experiments guidelines.

Patient consent for publication

Not applicable.

Competing interests

The authors declare that they have no competing interests.

References

1. World Health Organization (WHO): Global tuberculosis report 2020. WHO, Geneva, pp1-232, 2020.
2. Niehrs C: Function and biological roles of the Dickkopf family of Wnt modulators. Oncogene 25: 7469-7481, 2006.
3. Bee C, Abdiche YN, Stone DM, Collier S, Lindquist KC, Pinkerton AC, Pons J and Rajpal A: Exploring the dynamic range of the kinetic exclusion assay in characterizing antigen-antibody interactions. PLoS One 7: e36261, 2012.
4. Kim MS, Lee HN, Kim HJ and Myung SC: Single nucleotide polymorphisms in DKK3 gene are associated with prostate cancer risk and progression. Int Braz J Urol 41: 869-897, 2015.
5. Shao YC, Wei Y, Liu JF and Xu XY: The role of Dickkopf family in cancers: From bench to bedside. Am J Cancer Res 7: 1754-1768, 2017.
6. Xu J, Sadahira T, Kinoshita R, Li SA, Huang P, Wada K, Araki M, Ochiai K, Noguchi H, Sakaguchi M, *et al*: Exogenous DKK-3/REIC inhibits Wnt/β-catenin signaling and cell proliferation in human kidney cancer KPK1. Oncol Lett 14: 5638-5642, 2017.
7. Yang Y, Xu W, Zheng Z and Cao Z: LINC00459 sponging miR-218 to elevate DKK3 inhibits proliferation and invasion in melanoma. Sci Rep 9: 19139, 2019.
8. Khan Z, Arafah M, Shaik JP, Mahale A and Alanazi MS: High-frequency deregulated expression of Wnt signaling pathway members in breast carcinomas. Onco Targets Ther 11: 323-335, 2018.

9. Gebert LFR and MacRae IJ: Regulation of microRNA function in animals. Nat Rev Mol Cell Biol 20: 21-37, 2019.
10. Lei SL, Zhao H, Yao HL, Chen Y, Lei ZD, Liu KJ and Yang Q: Regulatory roles of microRNA-708 and microRNA-31 in proliferation, apoptosis and invasion of colorectal cancer cells. Oncol Lett 8: 1768-1774, 2014.
11. Peng G, Yang C, Liu Y and Shen C: miR-25-3p promotes glioma cell proliferation and migration by targeting FBXW7 and DKK3. Exp Ther Med 18: 769-778, 2019.
12. Huo J, Zhang Y, Li R, Wang Y, Wu J and Zhang D: Upregulated MicroRNA-25 mediates the migration of melanoma cells by targeting DKK3 through the WNT/β-catenin pathway. Int J Mol Sci 17: 1124, 2016.
13. Peng WX, Koirala P and Mo YY: LncRNA-mediated regulation of cell signaling in cancer. Oncogene 36: 5661-5667, 2017.
14. Hu Q, Ye Y, Chan LC, Li Y, Liang K, Lin A, Egranov SD, Zhang Y, Xia W, Gong J, *et al*: Oncogenic lncRNA downregulates cancer cell antigen presentation and intrinsic tumor suppression. Nat Immunol 20: 835-851, 2019.
15. Liu X, Fu Q, Li S, Liang N, Li F, Li C, Sui C, Dionigi G and Sun H: LncRNA FOXD2-AS1 functions as a competing endogenous RNA to regulate TERT expression by sponging miR-7-5p in thyroid cancer. Front Endocrinol (Lausanne) 10: 207, 2019.
16. Zhang XF, Ye Y and Zhao SJ: LncRNA Gas5 acts as a ceRNA to regulate PTEN expression by sponging miR-222-3p in papillary thyroid carcinoma. Oncotarget 9: 3519-3530, 2017.
17. Liu K, Liu C and Zhang Z: lncRNA GAS5 acts as a ceRNA for miR-21 in suppressing PDGF-bb-induced proliferation and migration in vascular smooth muscle cells. J Cell Biochem 120: 15233-15240, 2019.
18. Wang J, Liu X, Wu H, Ni P, Gu Z, Qiao Y, Chen N, Sun F and Fan Q: CREB up-regulates long non-coding RNA, HULC expression through interaction with microRNA-372 in liver cancer. Nucleic Acids Res 38: 5366-5383, 2010.
19. Li J, Han L, Roebuck P, Diao L, Liu L, Yuan Y, Weinstein JN and Liang H: TANRIC: An interactive open platform to explore the function of lncRNAs in cancer. Cancer Res 75: 3728-3737, 2015.
20. Nokin MJ, Durieux F, Peixoto P, Chiavarina B, Peulen O, Blomme A, Turtoi A, Costanza B, Smargiasso N, Baiwir D, *et al*: Methylglyoxal, a glycolysis side-product, induces Hsp90 glycation and YAP-mediated tumor growth and metastasis. Elife 5: e19375, 2016.
21. Li Y, Li H and Wei X: Long noncoding RNA LINC00261 suppresses prostate cancer tumorigenesis through upregulation of GATA6-mediated DKK3. Cancer Cell Int 20: 474, 2020.
22. Livak KJ and Schmittgen TD: Analysis of relative gene expression data using real-time quantitative PCR and the 2(-Delta Delta C(T)) method. Methods 25: 402-408, 2001.
23. Institute of Laboratory Animal Resources (U.S.), Committee on Care and Use of Laboratory Animals, National Institutes of Health (U.S.), Division of Research Resources: Guide for the Care and Use of Laboratory Animals. U.S. Dept. of Health and Human Services, Public Health Service, National Institutes of Health, Bethesda, MD, 1985.
24. Kilkenny C, Browne W, Cuthill IC, Emerson M and Altman DG; National Centre for the Replacement, Refinement and Reduction of Amimals in Research: Animal research: Reporting in vivo experiments-the ARRIVE guidelines. J Cereb Blood Flow Metab 31: 991-993, 2011.
25. Tetsu O and McCormick F: Beta-catenin regulates expression of cyclin D1 in colon carcinoma cells. Nature 398: 422-426, 1999.
26. Lodygin D, Epanchintsev A, Menssen A, Diebold J and Hermeking H: Functional epigenomics identifies genes frequently silenced in prostate cancer. Cancer Res 65: 4218-4227, 2005.
27. Sato H, Suzuki H, Toyota M, Nojima M, Maruyama R, Sasaki S, Takagi H, Sogabe Y, Sasaki Y, Idogawa M, *et al*: Frequent epigenetic inactivation of DICKKOPF family genes in human gastrointestinal tumors. Carcinogenesis 28: 2459-2466, 2007.
28. Hsieh SY, Hsieh PS, Chiu CT and Chen WY: Dickkopf-3/REIC functions as a suppressor gene of tumor growth. Oncogene 23: 9183-9189, 2004.
29. Kurose K, Sakaguchi M, Nasu Y, Ebara S, Kaku H, Kariyama R, Arao Y, Miyazaki M, Tsushima T, Namba M, *et al*: Decreased expression of REIC/Dkk-3 in human renal clear cell carcinoma. J Urol 171: 1314-1318, 2004.
30. Mao B, Wu W, Li Y, Hoppe D, Stannek P, Glinka A and Niehrs C: LDL-receptor-related protein 6 is a receptor for Dickkopf proteins. Nature 411: 321-325, 2001.
31. Zhang W, Shi S, Jiang J, Li X, Lu H and Ren F: LncRNA MEG3 inhibits cell epithelial-mesenchymal transition by sponging miR-421 targeting E-cadherin in breast cancer. Biomed Pharmacother 91: 312-319, 2017.
32. Zhao W, Geng D, Li S, Chen Z and Sun M: LncRNA HOTAIR influences cell growth, migration, invasion, and apoptosis via the miR-20a-5p/HMGA2 axis in breast cancer. Cancer Med 7: 842-855, 2018.
33. Zhang Y, Li H, Cao R, Sun L, Wang Y, Fan S, Zhao Y, Kong D, Cui L, Lin L, *et al*: Suppression of Mir-708 promotes DKK3 to inhibit Wnt/β-catenin signaling pathway in adult B-ALL. Blood 128: 5090, 2016.
34. Katoh M and Katoh M: WNT signaling pathway and stem cell signaling network. Clin Cancer Res 13: 4042-4045, 2007.
35. Zhan T, Rindtorff N and Boutros M: Wnt signaling in cancer. Oncogene 36: 1461-1473, 2017.
36. Ganesan K, Ivanova T, Wu Y, Rajasegaran V, Wu J, Lee MH, Yu K, Rha SY, Chung HC, Ylstra B, *et al*: Inhibition of gastric cancer invasion and metastasis by PLA2G2A, a novel beta-catenin/TCF target gene. Cancer Res 68: 4277-4286, 2008.